Lawrence Berkeley National Laboratory
Recent Work

Title
QUANTUM NUMBERS and DECAY MODES OF THE RESONANCES (3095) and (3684)

Permalink
https://escholarship.org/uc/item/68t28105

Author
Boyarski, A.M.

Publication Date
1975-06-01

QUANTUM NUMBERS AND DECAY MODES OF THE RESONANCES ψ (3095)

AND ψ' (3684)

June 1975

RECEIVED

14

DISCLAIMER

QUANTUM NUMBERS AND DECAY MODES OF THE RESONANCES ψ(3095) AND ψ(3684)[*]

A. M. Boyarski, M. Breidenbach, F. Bulos, G. J. Feldman, G. E. Fischer, D. Fryberger, G. Hanson, D. L. Hartill, B. Jean-Marie, R. R. Larsen, D. Lüke, V. Lüth, H. L. Lynch, D. Lyon, C. C. Morehouse, J. M. Paterson, M. L. Perl, T. P. Pun, P. Rapidis, B. Richter, R. F. Schwitters, W. Tanenbaum, and F. Vannucci

Stanford Linear Accelerator Center, Stanford University, Stanford, California 94305, USA.

G. S. Abrams, D. D. Briggs, W. Chinowsky, C. E. Friedberg, G. Goldhaber, J. A. Kadyk, A. M. Litke, B. A. Lulu, F. M. Pierre, B. Sadoulet, G. H. Trilling, J. S. Whitaker, F. Winkelmann, and J. E. Wiss

Lawrence Berkeley Laboratory and Department of Physics, University of California, Berkeley, California 94720, USA.

(Presented by V. Lüth)

1. INTRODUCTION

The recent months since the discovery of the new narrow resonances, named ψ(3095) and ψ(3684), at SLAC[1,2] and BNL[3] have been very exciting and exhilarating for particle physics. The experimental evidence is unmistakable. Furthermore, the ψ particles are clearly something new and unexpected, and they cannot be accommodated in our present classification scheme for elementary particles. A large number of experiments in different high energy laboratories have verified the existence of these particles and are searching for other particles that may be related to them. This report will summarize the results that have been obtained from an extensive analysis of decays of the ψ particles that were recorded by the SLAC-LBL solenoidal magnetic detector at SPEAR. A considerable fraction of these results have not been published and are to be taken as preliminary.

2. APPARATUS

The experiment is performed at the SLAC e^+e^- colliding beam facility, SPEAR.[4] This storage ring circulates one bunch of electrons and one bunch of positrons in a single magnetic guide field. The bunches collide at $0°$, alternately in two interaction regions that extend a few millimeters transverse and a few centimeters longitudinal to the beam. The beam energies may at present be varied between 1.5 GeV and 3.8 GeV. The energy resolution increases quadratically with energy, and is of the order of 1 MeV (standard deviation) for a center-of-mass energy of 3 GeV. It is dominated by fluctuations in the emission of synchrotron light. The absolute energy of the machine is known to about 0.1%. The calibration is based on measurements of the magnetic guide field and particle orbits.

The SLAC-LBL magnetic detector is schematically shown in Figure 1.[5] The solenoidal magnet provides a nearly uniform axial magnetic field of 4 kG in a volume 3 m long and 3 m in diameter. A particle leaving the interaction region in the center will first traverse the 0.15 mm stainless steel vacuum chamber and a pair of cylindrical scintillation counters that form an element of the trigger system. Continuing outwards, it will enter 4 sets of cylindrical wire spark chambers, 2 gaps each, with magnetostrictive readout. Next, the trigger hodoscope will provide time-of-flight information with a resolution of 0.5 nsec, thus allowing π/K separation up to 600 MeV/c momentum. Outside the 1 radiation length magnet coil an array of lead-scintillator shower counters (5 radiation lengths)

will identify electrons. Most hadrons will be absorbed in the 20 cm thick iron yoke and will not reach a set of spark chambers on the outside which aids muon identification. The detector covers a solid angle of 65% of 4π, the azimuthal acceptance is complete, and the subtended polar angle ranges from 50° to 130°. A hardware trigger requires at least two particles with momenta above 200 MeV/c. Consequently, totally neutral final states cannot be recorded. The data analysis constructs tracks, momenta, and vertices from the spark chamber information and selects three classes of events, i.e., the reactions $e^+e^- \to$ hadrons, $e^+e^- \to \mu^+\mu^-$, and $e^+e^- \to e^+e^-$. A hadronic event is required to have 3 or more tracks or 2 tracks that are acoplanar by more than 20°. Lepton pairs are required to have 2 collinear tracks, each carrying more than 50% of the beam energy. e-pairs are distinguished from μ-pairs using shower counter pulse heights. The background due to beam-gas interactions is determined from longitudinal distributions of reconstructed event vertices. Background contributions to the resonances are very small, less than 0.1%; they amount to roughly 5% outside the resonance region.

The luminosity is monitored by two pairs of small counters measuring Bhabha scattering at 25 mrad where the scattering is dominated by space-like photons, and consequently very weakly affected by resonance production.

3. SEARCH FOR NARROW RESONANCES

Shortly after the discovery of the $\psi(3095)$ a systematic search for other narrow resonances in e^+e^- annihilation was begun.[6] For this purpose the center-of-mass energy (twice the beam energy) was automatically increased by 1.9 MeV every few minutes, allowing for an average of 2 hadronic events per step. Data taken during each step were analyzed in real time and the relative cross sections were evaluated at the end of each step. During the first run of this search the $\psi(3684)$ was discovered. The scan was continued to cover the range from 3.2 GeV to 5.9 GeV, as shown in Fig. 2, and has recently been extended to 7.60 GeV. For technical reasons the region below 3.2 GeV has not been completed. Upper limits on the integrated cross section for the production of narrow resonances are presented in Table I. For comparison, the integrated cross section of the $\psi(3684)$ is of the order of 3700 nb MeV; thus the upper limits range from 12% to 25% of the $\psi(3684)$ cross section, with a sensitivity decreasing as the resonance width increases.

TABLE I

Results of the search for narrow resonances. Upper limits (90% confidence level) for the radiatively corrected integrated cross section of a possible narrow resonance. The width of this resonance is assumed to be small compared to the mass resolution.

Mass Range (GeV)	Limit on $\int \sigma_H \, dE_{cm}$ (nb MeV)
3.20 → 3.50	970
3.50 → 3.69	780
3.72 → 4.00	850
4.00 → 4.40	620
4.40 → 4.90	580
4.90 → 5.40	780
5.40 → 5.90	800
5.90 → 7.60	450

4. TOTAL AND LEPTONIC DECAY WIDTH OF THE $\psi(3095)$ AND $\psi(3684)$

Extensive measurements of the cross sections for the production of hadrons, μ-pairs, and e-pairs have been made as a function of the c.m. energy near both ψ resonances.[7,8] The data are presented in Figs. 4 and 5. Contrary to the hadron data the lepton data are not corrected for the loss of events with $|\cos\theta| > 0.6$, where θ is the angle between the outgoing positive lepton and the incident positron. The analysis of $\psi(3684)$ data revealed a structure in the invariant mass of the lepton pairs which is due to the decay of the $\psi(3684)$ into the $\psi(3095)$ and a subsequent leptonic decay of this state. The cuts applied to remove this contamination of collinear lepton pairs lead to an additional 5% loss of events. The cuts are illustrated by the dashed line in Fig. 3.

The most striking feature of the data is the copious production of hadrons, the sizable lepton pair-production at the $\psi(3095)$, and the widths of the distributions, which are compatible with the experimental resolution. A machine independent value for the resonant hadronic cross sections can be obtained by integration over energy.

$$\psi(3095): \quad \int \sigma_H^\psi(E)\,dE = 10400 \pm 1500 \text{ nb MeV}$$

$$\psi(3684): \quad \int \sigma_H^\psi(E)\,dE = 3700 \pm 600 \text{ nb MeV}$$

These integrals are corrected for the considerable effects of initial state radiation.[9]

In order to determine the exact mass m, and Γ_e, Γ_μ, Γ_H, the partial widths into electrons, muons, and hadrons, respectively, the 3 data sets for each resonance were fitted simultaneously. The total decay width is defined as $\Gamma = \Gamma_e + \Gamma_\mu + \Gamma_H$, thus assuming that there are no unobserved decay modes. Assuming further that the ψ's have Breit-Wigner shape, then for any decay mode f the cross section σ_f for the reaction $e^+e^- \to \psi \to f$ may be written as follows,

$$\sigma_f = \frac{(2J+1)\pi}{E^2} \frac{\Gamma_e \Gamma_f}{(M-E)^2 + \Gamma^2/4} \ .$$

Here, J is the spin of the ψ, Γ is its total width, Γ_f is its partial decay width to the state f and E is the c.m. energy. The fit folds the beam resolution function with radiative effects and the resonance σ_f. Furthermore, for each of the 3 decay modes it adds the direct channel $e^+e^- \to f$ and possible interference between these amplitudes. It assumes J = 1 and an angular distribution of $1 + \cos^2\theta$ for the leptonic decay. The results[10] are given in Table II with errors that reflect our systematic uncertainties. They include energy setting errors of ± 100 keV, $\pm 3\%$ errors in overall normalization, and $\pm 15\%$ for uncertainties in the detection efficiency for the hadronic decays. For the $\psi(3095)$ a comparison between Γ_e and Γ_μ constitutes a sensitive test of μ-e universality.

5. J^{PC} ASSIGNMENT OF $\psi(3105)$ AND $\psi(3684)$

The fact that the ψ resonances are produced in e^+e^--annihilation may suggest that they couple directly to photons and thus have the same spin, parity, and charge conjugation, $J^{PC} = 1^{--}$. This quantum number assignment can be tested by looking for an interference between the resonant and the QED amplitudes and by examination of the angular distribution of leptons from ψ decays. Interference is studied in the $\mu^+\mu^-$ channel rather than in the e^+e^- channel that is dominated by the t-channel QED amplitude. To exhibit interference effects it is convenient to use the ratio of $\mu^+\mu^-$ to e^+e^- yields as a function of c.m. energy. This ratio minimizes normalization errors in the data and is most sensitive to the interference, because the electron amplitudes interfere constructively for energies below the resonance, where the muon amplitudes are expected to show destructive

TABLE II

Properties of the ψ-particles as obtained from fit to cross sections
σ_{HAD}, $\sigma_{\mu\mu}$, and σ_{ee}

	$\psi(3095)$	$\psi(3684)$
Mass	3.095 ± 0.004 GeV	3.684 ± 0.005 GeV
J^{PC}	1^{--}	1^{--}
$\Gamma_e = \Gamma_\mu$	4.8 ± 0.6 keV	2.2 ± 0.3 keV
Γ_H	59 ± 14 keV	220 ± 56 keV
Γ	69 ± 15 keV	225 ± 56 keV
Γ_e/Γ	0.069 ± 0.009	0.0097 ± 0.0016
Γ_H/Γ	0.86 ± 0.02	0.981 ± 0.003
Γ_μ/Γ_e	1.00 ± 0.05	0.89 ± 0.16

interference. The data for both resonances are presented in Fig. 6 and compared to curves calculated for no interference, e.g., $J = 0$, and maximum interference, i.e., a pure $J^{PC} = 1^{--}$ state. The data agree with the maximum interference prediction. The $\psi(3095)$ measurements disagree with the no interference hypothesis by 2.7 standard deviations, and the $\psi(3684)$ data deviate by 4.9 standard deviations from the no interference curve. Furthermore the angular distributions of e-pairs and μ-pairs, after subtraction of the QED contributions, are consistent with a $1 + \cos^2\theta$ behavior expected for a simple $J^{PC} = 1^{--}$ state, but inconsistent with 2^{--} and 3^{--} states.

The assumption that the resonance is an eigenstate of P and C has been tested by studying the front-back asymmetry for μ-pairs across the resonances. The absence of any large asymmetry indicates no significant violation of parity or charge conjugation. It argues against the possibility of the ψ's not being eigenstates of P and C or being a degenerate mixture of states of opposite P or C.

Thus, the angular distributions confirm the interference result that both ψ resonances have the same quantum numbers as the photon, $J^{PC} = 1^{--}$.

## 6. HADRONIC DECAY MODES OF THE $\psi(3095)$

A detailed analysis of the exclusive hadronic final state has been under way for some time to determine the G-parity and the isospin of the $\psi(3095)$ from the all-pion decay modes and to test the SU_3 character of this state.

6.1 G-parity of the $\psi(3095)$

Since the shower counter system had not been designed to have reasonable energy resolution and the time-of-flight system limits particle mass assignment to low momenta, the identification of exclusive multiparticle final states relies on kinematics. Using the measured momenta and angles of the charged tracks in the detector energy and momentum conservation is tested for each event. Fig. 8 shows the sum of the energies of all charged particles in 4-prong events with zero total charge and balanced momenta. The "true" 4π final states accumulate at a c.m. energy around 3.1 GeV; the broad enhancement below is due to decays $\psi \to \pi^+\pi^-K^+K^-$. The number of 4π final states in the data is determined from the Monte Carlo fit to the data that includes all possible contaminations by other decays. Similarly, the number of the all-pion final states with one missing π^0 is extracted from a fit to the missing mass distribution. As an example, the square of the mass recoiling against four charged pions is shown in Fig. 9 for data taken on and off the resonance. The difference is quite

dramatic; apart from that, the data prove that the $\psi(3095)$ decays into both even and odd numbers of pions, a violation of G-parity. However, this violation can be explained if the resonance couples to a photon.

Consider the diagrams involved in hadron production at the $\psi(3095)$ and outside the resonance region

(1)   (2)   (3)
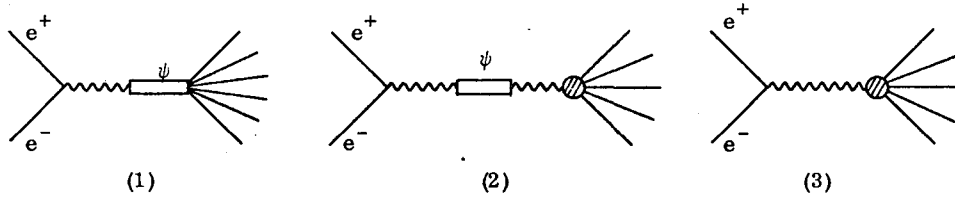
and compare them to μ-pair production

(4)   (5)
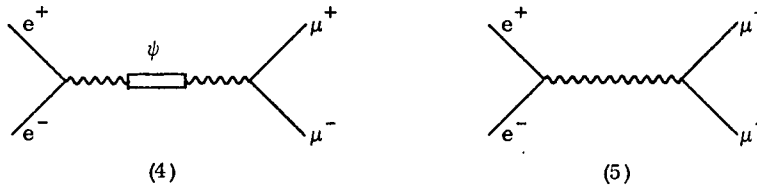
Graph (1) describes the direct decay of the ψ into hadrons, whereas (2) and (3) show the production of hadrons via an intermediate photon. The final states in (2) must be the same as the nonresonant final states in (3). These states need not conserve G-parity and may be different from the states produced by (1). Furthermore, the ratio of hadron to μ-pair production for diagrams (3) and (5), i.e., off resonance, must be the same as for diagrams (2) and (4), i.e., on resonance. Thus, if the hadronic events observed are due to the second order electromagnetic process (2) only, the following relation holds:

$$R_{on} = \frac{\sigma^H_{on}}{\sigma^\mu_{on}} = \frac{\sigma^H_{off}}{\sigma^\mu_{off}} = R_{off} .$$

To test this hypothesis the ratios of all-pion cross sections to μ-pair cross sections are compared for data at 3.0 GeV and at the $\psi(3095)$. The ratio $\alpha = R_{on}/R_{off}$ is shown in Fig. 10 for different pion multiplicities. This variable is most insensitive to systematic errors and inefficiencies. The production of an even number of pions is consistent with a coupling of the $\psi(3095)$ to an intermediate photon, whereas most of the odd pion states come from direct decays of the $\psi(3095)$. Consequently the $\psi(3095)$ appears to have odd G-parity.

The contribution of the hadronic decays via an intermediate photon can be derived as $B_{\gamma h} = B_{\mu\mu}R$ and amounts to 18% of the total width, whereas the direct decays contribute 68%, and the lepton decays 14% to the total width.

6.2 Isospin of the $\psi(3095)$

Knowing that the G-parity and the charge conjugation of the $\psi(3095)$ are odd, the isospin has to be even, i.e., 0 or 2. The analysis of the $\pi^+\pi^-\pi^0$ decay, which is mostly a direct hadronic decay of the $\psi(3095)$, reveals that this state is dominantly produced as $\rho\pi$. This can be verified from the Dalitz plot in Fig. 11. The different charge states of the $\rho\pi$ system are equally frequent and clearly

favor the I = 0 assignment.

An even stronger[11] argument for I = 0 is derived from the observation of the decay $\psi(3095) \rightarrow$ $\rightarrow p\bar{p}$ with a branching ratio of $(0.20 \pm 0.04)\%$, which is far above the expected electromagnetic rate. The $p\bar{p}$ final states are clearly separated by kinematics from the $\mu^+\mu^-$ pairs as shown in Fig. 12. Since a $p\bar{p}$ can only be in an I = 0 or I = 1 state, and G = -1 excludes I = 1, the $\psi(3095)$ must be an I = 0 state.

6.3 $\underline{SU_3 \text{ character of the } \psi(3095)}$

Since the $\psi(3095)$ seems to decay like a nonstrange meson with I = 0, the question arises whether or not the resonance is an SU_3 singlet, the eighth component of an octet, or a mixture of the two, such as the physical ω and ϕ states. For an SU_3 singlet, all decays into two members of the same multiplet are forbidden, for instance $\psi \rightarrow K^+K^-$, or $\psi \rightarrow K_S K_L$. For the eighth component of an octet these decays are permitted with equal rates, whereas exact SU_3 predicts that in second order electromagnetic decays via a photon the decays $\psi \rightarrow \pi^+\pi^-$ and $\psi \rightarrow K^+K^-$ occur at equal rates, but $\psi \rightarrow K_S K_L$ is forbidden.[12] Some detailed study of the production of quasi two-body states of strange mesons seems to support the hypothesis that the $\psi(3095)$ is an SU_3 singlet. The most stringent limit has been set on the branching ratio for $\psi \rightarrow K_S K_L$. One event for this mode, possibly background, leads to a 90% confidence limit of 2×10^{-4}.

Another test of the singlet hypothesis can be derived from decays into baryon pairs. For events with identified decays of Λ and $\bar{\Lambda}$, the momentum of the Λ is plotted versus the momentum of the $\bar{\Lambda}$ in Fig. 13. A kinematic fitting procedure selects 19 ± 5 $\Lambda\bar{\Lambda}$ final states with momenta of 1080 MeV. Thus, the branching ratio to $\Lambda\bar{\Lambda}$ of $(0.16 \pm 0.08)\%$ is of the same order of magnitude as the branching ratio to $p\bar{p}$.

6.4 Other decay modes of the $\psi(3095)$

The study of the decay modes of the $\psi(3095)$ is still in progress. The decays that have been identified so far are listed in Table III. Most of the results should be considered preliminary and some of the errors quoted have been doubled to cover the systematic uncertainties. So far there is no strong evidence for radiative decays. The decay $\psi(3095) \rightarrow \pi^+\pi^+\pi^-\pi^-\pi^0$, for example, could contain some contamination from $\psi(3095) \rightarrow \pi^+\pi^+\pi^-\pi^-\gamma$. The observation of a large contribution from $\omega\pi^+\pi^-$ and $\rho\pi\pi\pi$, as well as the distribution of the missing mass in Fig. 9, indicates, however, that the radiative decay cannot be a major one.

7. HADRONIC DECAYS OF THE $\psi(3684)$

As the decay of the $\psi(3684)$ is dominated by the cascade into the $\psi(3095)$,[13] the study of all other decay modes is rather difficult and just beginning.

7.1 Decays $\psi(3684)$ to $\psi(3095)$

The presence of the $\psi(3095)$ among the decay products of the $\psi(3684)$ is detectable in two ways. First, the study of μ-pairs[14] revealed two well-separated peaks in the invariant mass distribution, as shown in Fig. 3b, one corresponding to μ-pairs produced at full energy, i.e., direct $\mu^+\mu^-$ production plus the decays $\psi(3684) \rightarrow \mu^+\mu^-$, and one around 3.1 GeV from the process

$$\psi(3684) \rightarrow \psi(3095) + X.$$
$$ \hookrightarrow \mu^+\mu^-$$

TABLE III

Decay Modes of the $\psi(3095)$

Mode	Branching Ratio (%)	No. of Events Observed	Comments
e^+e^-	6.9 ± 0.9	ca 2000	
$\mu^+\mu^-$	6.9 ± 0.9	ca 2000	
$\rho\pi$	1.3 ± 0.3	153 ± 13	$>70\%$ of $\pi^+\pi^-\pi^0$
$2\pi^+ 2\pi^-$	0.4 ± 0.1	76 ± 9	
$2\pi^+ 2\pi^- \pi^0$	4.0 ± 1.0	675 ± 40	$\begin{cases} 20\% \omega\pi^+\pi^- \\ 30\% \rho\pi\pi\pi \end{cases}$
$3\pi^+ 3\pi^-$	0.4 ± 0.2	32 ± 7	
$3\pi^+ 3\pi^- \pi^0$	2.9 ± 0.7	181 ± 26	
$4\pi^+ 4\pi^- \pi^0$	0.9 ± 0.3	13 ± 4	
$\pi^+\pi^- K^+K^-$	0.4 ± 0.2	83 ± 18	$\begin{cases} \text{not including} \\ K^*(892) \; K^*(1420) \end{cases}$
$2\pi^+ 2\pi^- K^+K^-$	0.3 ± 0.1		
$K_S K_L$	< 0.02	≤ 1	90% C.L.
$K^0 K^{0*}(892)$	0.24 ± 0.05	57 ± 12	
$K^\pm K^{\mp*}(892)$	0.31 ± 0.07	87 ± 19	
$K^0 K^{0*}(1420)$	< 0.19	≤ 3	90% C.L.
$K^\pm K^{\mp*}(1420)$	< 0.19	≤ 3	90% C.L.
$K^{*0}(892)\bar{K}^{*0}(892)$	< 0.06	≤ 3	90% C.L.
$K^{*0}(1420)\bar{K}^{*0}(1420)$	< 0.18	≤ 3	90% C.L.
$K^{*0}(892)K^{*0}(1420)$	0.37 ± 0.10	30 ± 7	
$p\bar{p}$	0.21 ± 0.04	105 ± 11	$\begin{cases} \text{assuming} \\ f(\theta) \sim 1+\cos^2\theta \end{cases}$
$\Lambda\bar{\Lambda}$	0.16 ± 0.08	19 ± 5	
$\left.\begin{array}{l} p\bar{p}\,\pi^0 \\ \bar{n}p\pi^- \\ \bar{p}n\pi^+ \end{array}\right\}$	0.37 ± 0.19	87 ± 30	

A similar structure is observed in the 3-prong and 4-prong events. Taking into account the leptonic branching ratio of the $\psi(3095)$, the data yield

$$\frac{\Gamma(\psi(3684) \to \psi(3095) + \text{anything})}{\Gamma(\psi(3684) \to \text{all})} = 0.57 \pm 0.08 .$$

Alternatively, one observes the $\psi(3095)$ in the reaction

$$\psi(3684) \to \psi(3095) \pi^+ \pi^-$$

where the identification of the $\psi(3095)$ is made from its sharply defined mass. In Fig. 14a the missing mass recoiling against any pair of oppositely charged particles is shown. The $\psi(3095)$ signal above a smooth background has a width consistent with the experimental resolution and unambiguously identifies the decay mode. The observed rates, corrected for all known inefficiencies, lead to the branching ratio

$$\frac{\Gamma(\psi(3684) \to \psi(3095) \pi^+ \pi^-)}{\Gamma(\psi(3684) \to \text{all})} = 0.32 \pm 0.04 .$$

The errors include uncertainties in the ratio of the average detection efficiencies for hadronic decays of the two resonances and in the efficiency for observing both recoil pions.

The ratio of the two branching fractions measures

$$\frac{\Gamma(\psi(3684) \to \psi(3095) \pi^+ \pi^-)}{\Gamma(\psi(3684) \to \psi(3095) + \text{anything}} = 0.56 \pm 0.03 .$$

If the cascade decay of $\psi(3684)$ to $\psi(3095)$ proceeds entirely via the reaction $\psi(3684) \to \psi(3095)\pi\pi$, the above ratio would have roughly the values 2/3, 1, or 1/3 for $\pi\pi$ states of definite isospin 0, 1, or 2, respectively. Clearly, I = 0 is preferred. If one assumes that the $\psi(3684)$ like the $\psi(3095)$ decays to a pure isoscalar state, the difference between the measured and expected value may indicate that there are decay modes $\psi(3684) \to \psi(3095) + $ neutrals other than the $\psi(3095)\pi^0\pi^0$ with branching ratios $\leq 10\%$ of the total.

There seems to be some evidence for the decay

$$\psi(3684) \to \psi(3095)\eta$$

with a branching ratio of a few percent. This mode as well as radiative decays via an intermediate resonance, i.e.,

$$\psi(3684) \to X\gamma$$
$$\llcorner\!\longrightarrow \psi(3095)\gamma\gamma$$

has been studied. This will be discussed by G. Feldman.[15]

Figure 14b contains a subset of events that have both a lepton pair from the decay of the $\psi(3095)$ and the recoil pion pair. This sample has been used in a study of the angular distributions. Preliminary results indicate that the data are consistent with the hypothesis that the dipion state is a J = 0 state in an S-wave with respect to the lepton pair. If this is confirmed, it will independently establish the quantum numbers of the $\psi(3684)$ to be $J^{PC} = 1^{--}$.

Furthermore, this class of events proves that the $\psi(3684)$ is, apart from the Λ, the only particle that marks its decay pattern in proper Greek script.

7.2 Other decays of the $\psi(3684)$

The study of the remaining 43% of the decays of the $\psi(3684)$ is just beginning. As for the $\psi(3095)$, an attempt has been made to identify exclusive final states by means of kinematical constraints. A comparison of the kinematics of 4-prong events observed at the two ψ-states is presented in Fig. 15.

At the $\psi(3095)$ the 4-body final states are readily identified along the bottom line of diagram (a) and the $\pi^+\pi^+\pi^-\pi^-\pi^0$ states distinctly exhibit a linear correlation between the missing momentum and the total energy observed in the charged tracks. After the subtraction of the cascade decays in (c) from the total in (b), the direct decays of the $\psi(3684)$ in (d) show remarkably few distinct features. Up to now, no direct decay with a branching ratio of more than 1% has been seen. Upper limits for the decays into $\rho^0\pi^0$ and $\pi^+\pi^+\pi^-\pi^-\pi^0$ have been set and are listed in a summary in Table IV.

TABLE IV

Decay Modes of the $\psi(3684)$

Mode	Branching Ratio (%)	Comments
e^+e^-	0.97 ± 0.16	$\left.\vphantom{\begin{matrix}a\\b\end{matrix}}\right\}\mu\text{-e universality assumed}$
$\mu^+\mu^-$	0.97 ± 0.16	
$\psi(3095)$ anything	57 ± 8	
$\psi(3095)\,\pi^+\pi^-$	32 ± 4	$\left.\vphantom{\begin{matrix}a\\b\end{matrix}}\right\}$ these decays are included in
$\psi(3095)\,\eta$	4 ± 2	the fraction for ψ + anything
$\psi(3095)\,\gamma\gamma$	$< 6.6*$	via an intermediate state
$\rho^0\pi^0$	$< 0.1*$	
$2\pi^+ 2\pi^-\pi^0$	$< 0.7*$	
$p\bar{p}$	$< 0.03*$	

* 90% confidence limit based on a preliminary analysis

The suppression of decays into an odd number of pions is a remarkable property and may indicate that there is some mechanism that prevents the kind of decays that are most frequent at the $\psi(3095)$, or, in other words, a principle that favors decays with more than one neutral particle in the final state.

8. SUMMARY AND CONCLUSIONS

Though there may not be solid proof, there is evidence in favor of the hypothesis that the resonances observed in e^+e^- annihilation, $\psi(3095)$ and $\psi(3684)$, are hadrons.

(a) The ψ's decay directly to hadrons in a state of definite G-parity and isotopic spin,
$$G = -1, \quad I = 0.$$

(b) Parity and charge conjugation appear to be good quantum numbers; the spin is identical to the spin of the photon, $J^{PC} = 1^{--}$.

Furthermore, measurements of diffractive photoproduction of the ψ at SLAC[16,17] and FNAL[18] have determined a ψ-nucleon total cross section of ~ 1 mb.

The most remarkable property of the ψ resonances is their narrow widths, 69 keV for the $\psi(3095)$ and 225 keV for the $\psi(3684)$. Though it is not yet clear what theoretical framework will eventually incorporate the new particles, there are two general classes of theories that can suppress the decay of a hadron.[19,20] One possibility is that strong decays are inhibited by a dynamical mechanism based on the existence of a new additive quantum number. Charm is an example of such a scheme. In the charm picture the ψ particles are composed of a pair of charm-anticharm quarks and thus have charm zero. The verification of the charm scheme will probably require the proof of

the existence of charmed hadrons. At SPEAR a search for such particles has been performed and no evidence was found.[21] The second possibility implies that strong decays of the ψ particles are exactly forbidden by a new nonadditive quantum number. The various color models belong to this class. If the ψ's were colored states they would decay primarily through photon emission. So far, there is no strong evidence for radiative decays of the ψ particles.

Another surprising phenomenon that has been observed in e^+e^--annihilation is the variation of the fundamental quantity R, the ratio of $\sigma_T(e^+e^- \to \text{hadrons})$ to $\sigma(e^+e^- \to \mu^+\mu^-)$, the point cross section for muon pair production. The enhancement around 4.1 GeV[22] could either be a resonance or a threshold phenomenon related to the increase in R. There is, up to now, no evidence that the enhancement is actually a resonance, but little work has been done to clarify this point.

In any case, the basic question that remains unsolved is whether or not these two phenomena, the narrow width of the ψ particles and the increase in R, are related, and, if yes, how?

ACKNOWLEDGEMENT

We would like to thank F. J. Gilman and other members of the SLAC Theory Group for stimulating discussions.

REFERENCES

1) J.-E. Augustin et al., Phys. Rev. Letters 33, 1406 (1974).

2) G. S. Abrams et al., Phys. Rev. Letters 33, 1433 (1974).

3) J. J. Aubert et al., Phys. Rev. Letters 33, 1404 (1974). (These authors have named the particle J(3100).)

4) SPEAR Storage Ring Group, Proc. IXth Int. Conf. on High Energy Accelerators, Stanford Linear Accelerator Center, 1974, pp. 37-42.

5) J.-E. Augustin et al., Phys. Rev. Letters 34, 233 (1975).

6) A. M. Boyarski et al., Phys. Rev. Letters 34, 762 (1975).

7) A. M. Boyarski et al., Phys. Rev. Letters 34, 1357 (1975).

8) A. M. Boyarski et al., to be submitted to Phys. Rev. Letters.

9) D. R. Yennie, Phys. Rev. Letters 34, 239 (1975).

10) Results related to the ψ(3095) have been published by other groups, but the authors have not applied radiative corrections: W. W. Ash et al., Nuovo Cimento Letters 11, 704 (1974); R. Baldini-Celio et al., Nuovo Cimento Letters 11, 711 (1974); G. Barbiellini et al., Nuovo Cimento Letters 11, 718 (1974); W. Braunschweig et al., Phys. Letters 53B, 393 (1975).

11) W. Braunschweig et al., DESY-75-14 (1975).

12) H. J. Lipkin, Phys. Rev. Letters 31, 656 (1973).

13) G. S. Abrams et al., Phys. Rev. Letters 34, 1177 (1975).

14) The e-pairs are not used for this analysis because of the large background from the radiative tail of the Bhabha scattering (compare Fig. 3a).

15) G. J. Feldman, rapporteur's talk at this Conference.

16) J. T. Dakin et al., Phys. Letters 56B, 405 (1975).

17) U. Camerini et al., SLAC-PUB-1591 (1975), submitted to Phys. Rev. Letters.

18) B. Knapp et al., Phys. Rev. Letters 34, 1040 (1975); B. Knapp et al., Phys. Rev. Letters 34, 1044 (1975).

19) H. Harari, SLAC-PUB-1514 (1974), unpublished.

20) F. J. Gilman, SLAC-PUB-1537 (1975), to be published in Proc. of Orbis Scientiae II, Coral Gables, Florida, 1975.

21) A. M. Boyarski et al., SLAC-PUB-1583 (1975), submitted to Phys. Rev. Letters.

22) J.-E. Augustin et al., Phys. Rev. Letters 34, 764 (1975).

MUON SPARK CHAMBERS

FLUX RETURN

SHOWER COUNTERS

COIL

END CAP

TRIGGER COUNTERS

SPARK CHAMBERS

PIPE COUNTER

COMPENSATING SOLENOID

VACUUM CHAMBER

LUMINOSITY MONITOR

2292A1

} MUON WIRE CHAMBERS

} IRON (8 in.)

SHOWER COUNTERS (24)

COIL

TRIGGER COUNTERS (48)

CYLINDRICAL
WIRE CHAMBERS

$\vec{B}$

BEAM PIPE

TRIGGER
COUNTERS (2)

SUPPORT
POST (6)

1 meter
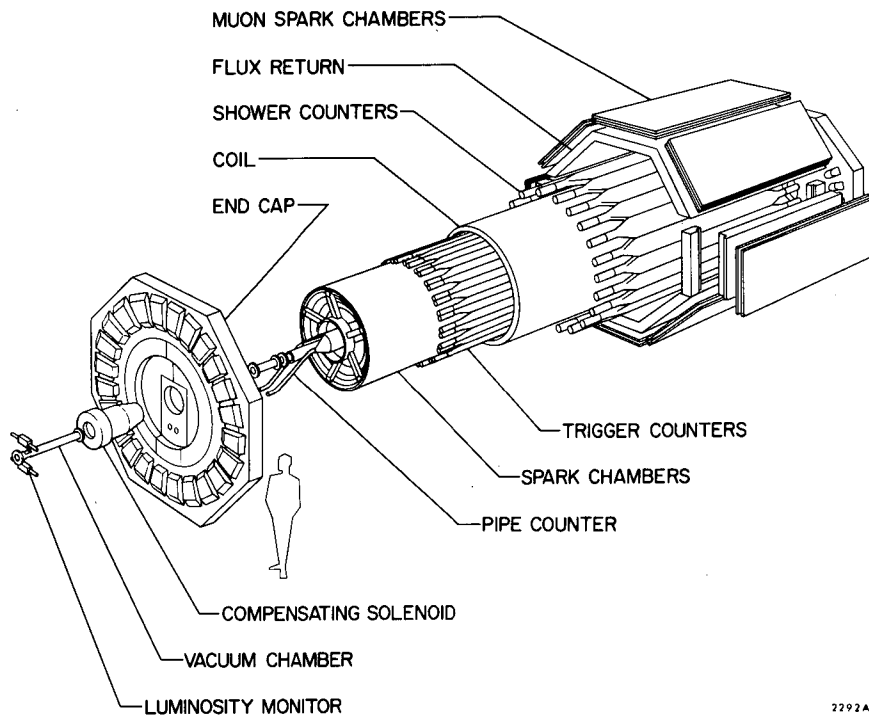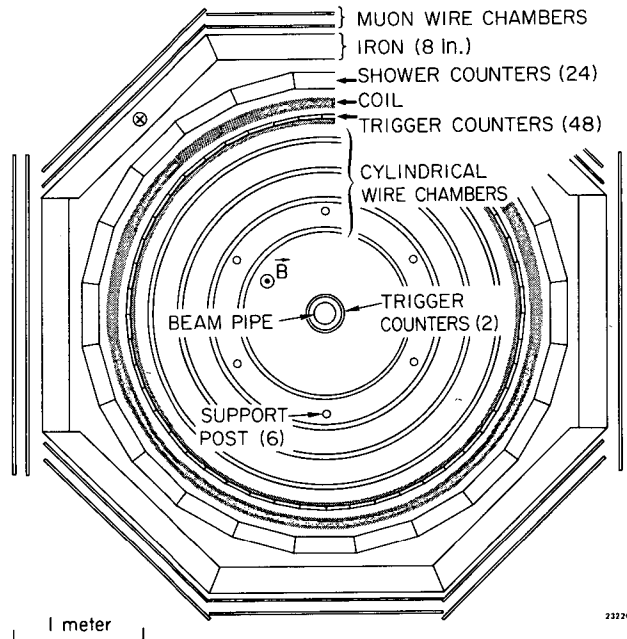
2322C3

Fig. 1   SLAC–LBL Magnetic Detector at SPEAR.

a) Telescoped view.
b) End view.
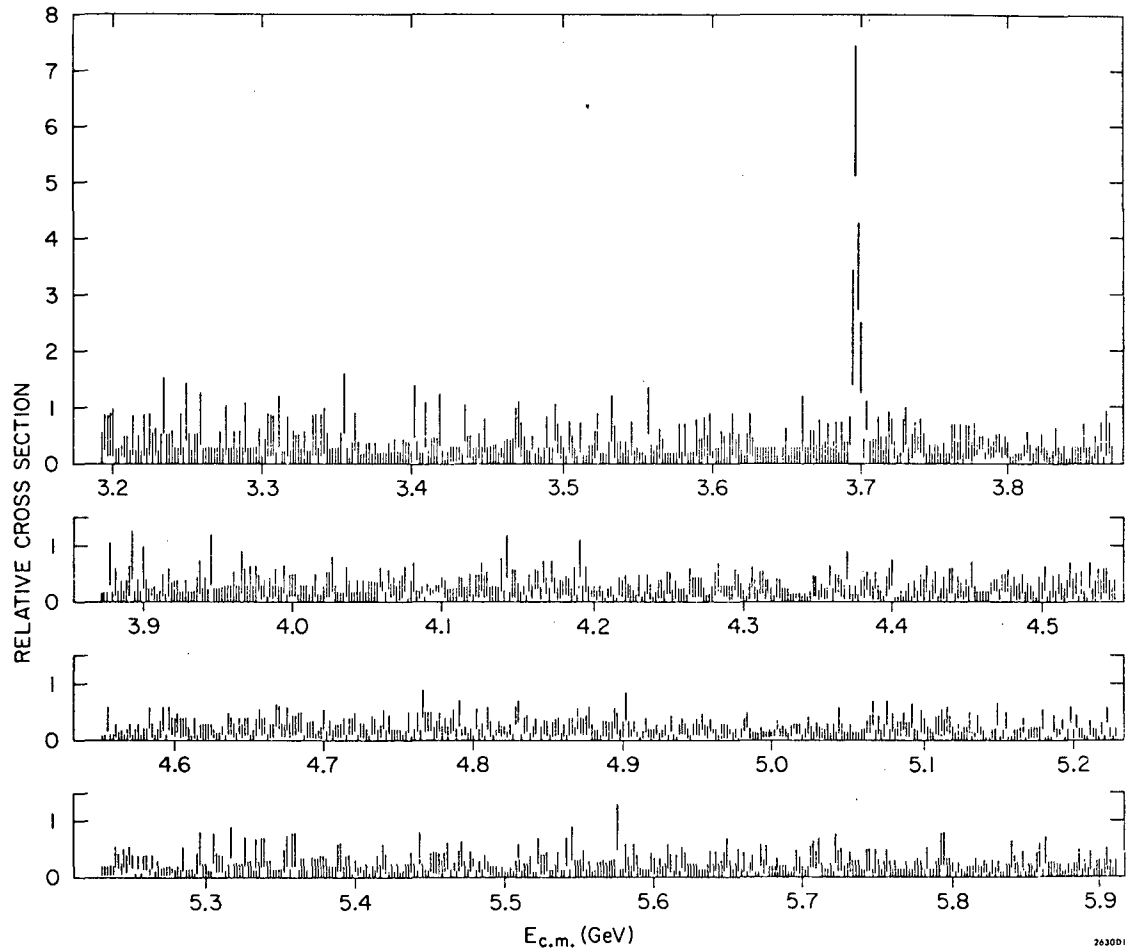
Fig. 2 Relative cross section for $e^+e^- \to$ hadrons as obtained from the fine mesh scan. The $\psi(3684)$ stands out clearly; it was first seen in the process of this scan. The energy scale shown is known to be miscalibrated by a factor of 1.003.
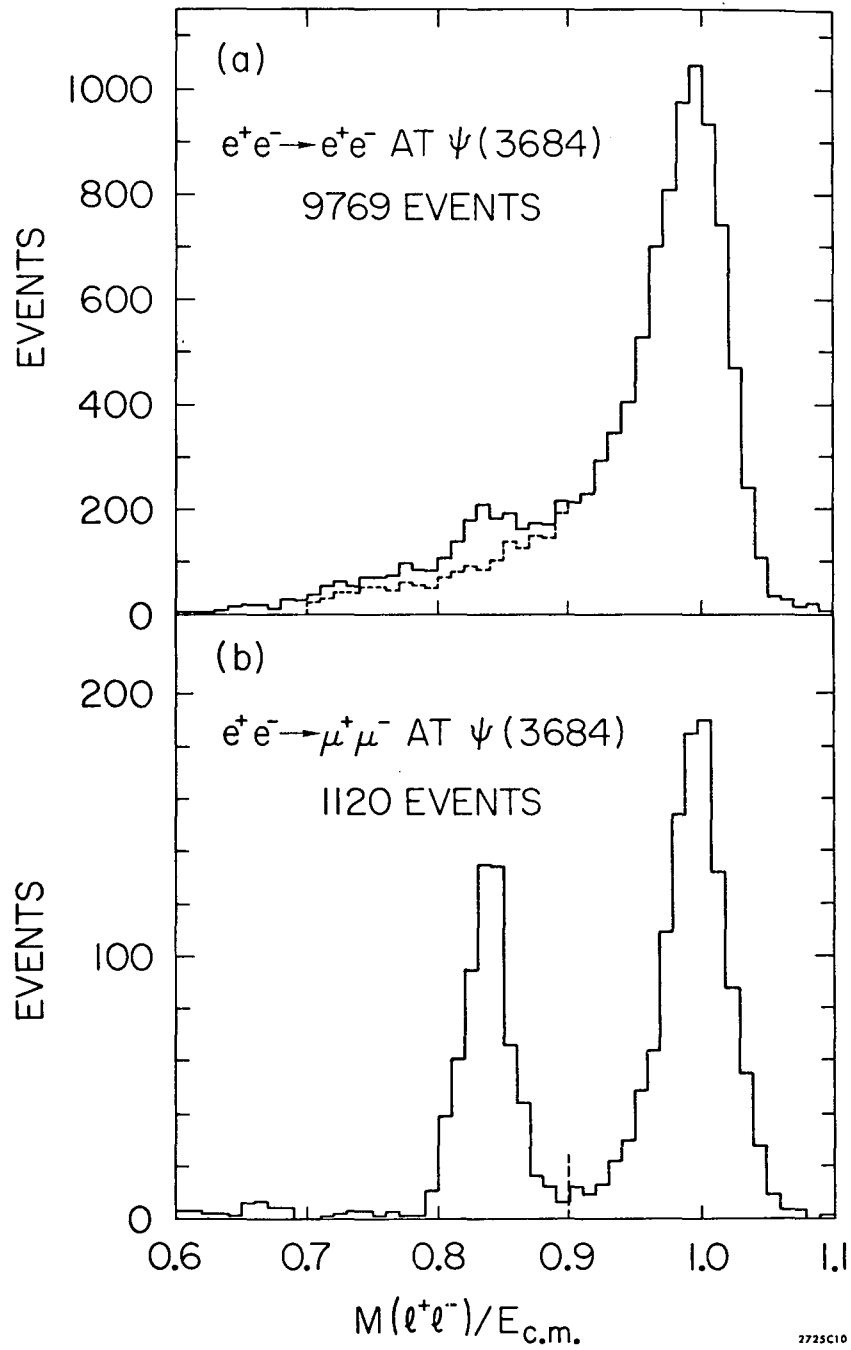
Fig. 3 Effective mass of lepton pairs, collinear to within 10^{0}, as observed at the $\psi(3684)$. The dotted line indicates the cuts made.
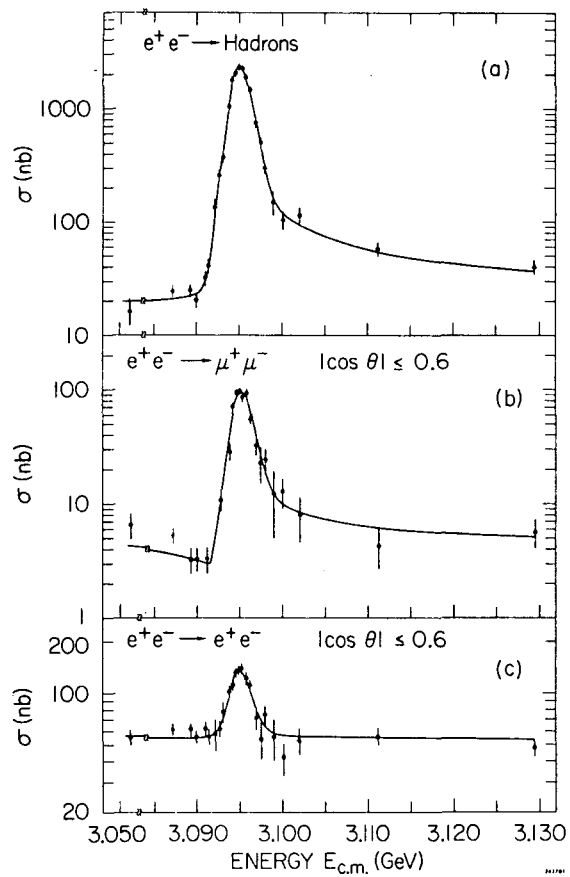
Fig. 4 Cross sections in the region of the ψ(3095). The errors given include systematics, but not the uncertainties in the overall normalization. The curves give the cross sections obtained in the fit and they account for radiative effects and limited resolution.
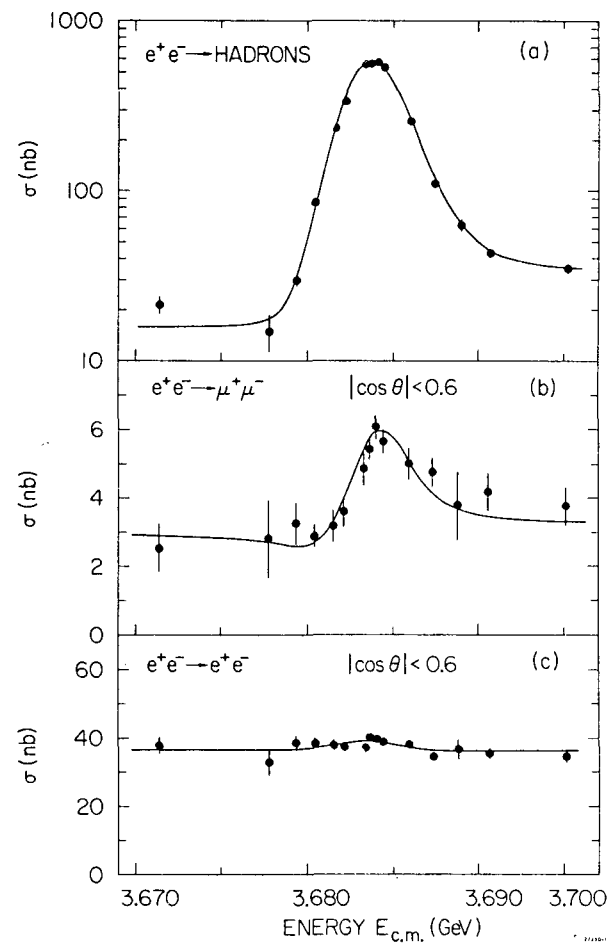
Fig. 5 Cross sections in the region of the ψ(3684).
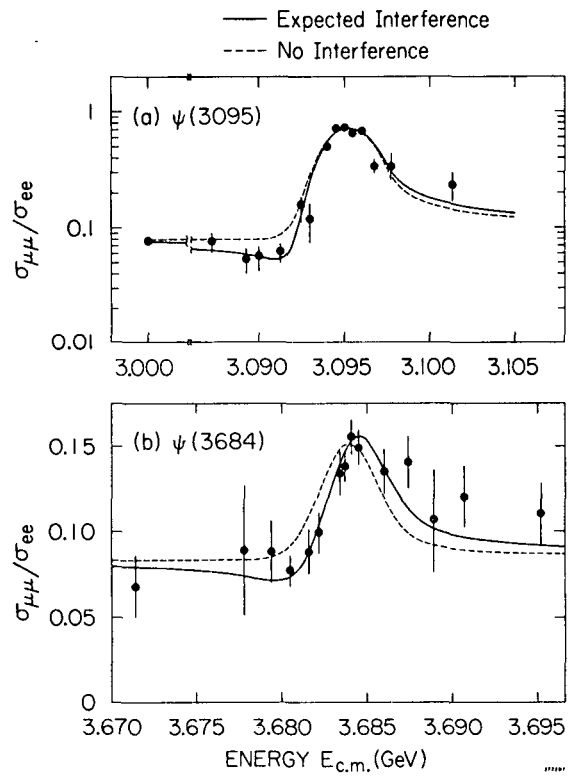
Fig. 6 The ratio of the μ-pair yield to e-pair yield as a function of c.m. energy. The dashed line gives the expected ratio for no interference; the solid line gives the ratio for full interference as obtained from the fit to the cross section data in Figs. 4 and 5.
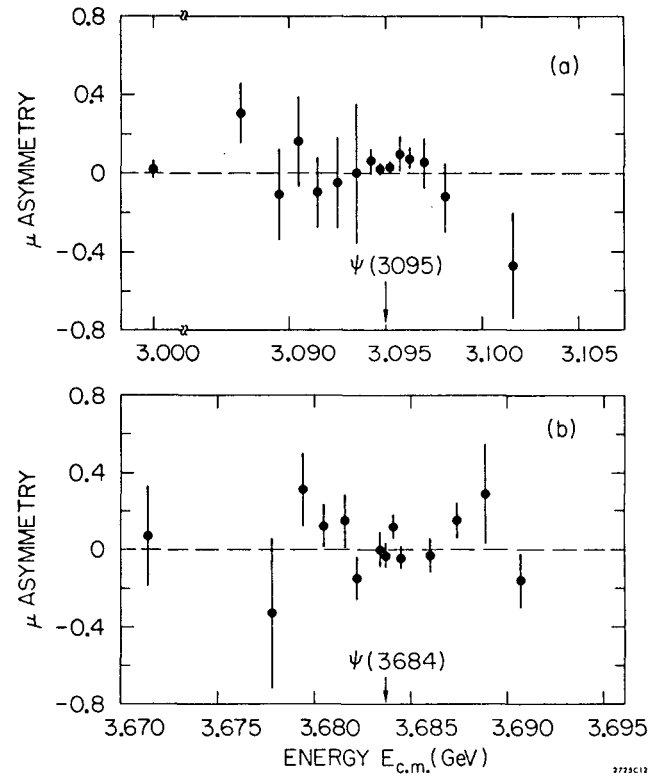
Fig. 7 The front-back asymmetry for μ-pairs as a function of c.m. energy.
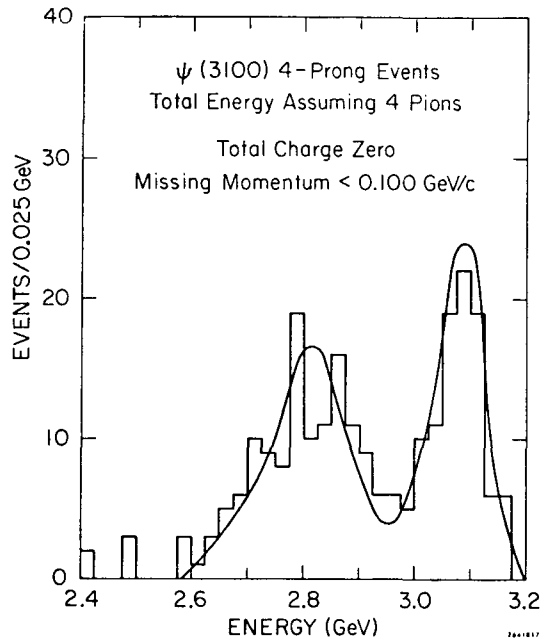
Fig. 8 Total energy observed in 4-prong events with a momentum imbalance of less than 100 MeV/c and total charge equal to zero, assuming all particles are pions. The curve shows a Monte Carlo fit to the data.

Fig. 9 The invariant mass squared recoiling against 4-charged pions

a) at 3.0 GeV.
b) at the $\psi(3095)$.

$$\alpha = \frac{R_{ON}}{R_{OFF}} = \frac{\sigma_{ON}^{H} / \sigma_{ON}^{\mu}}{\sigma_{OFF}^{H} / \sigma_{OFF}^{\mu}}$$
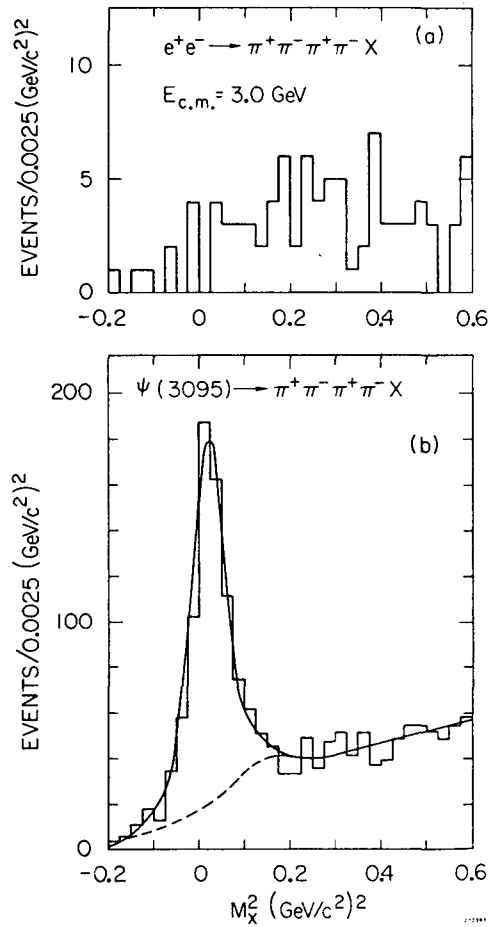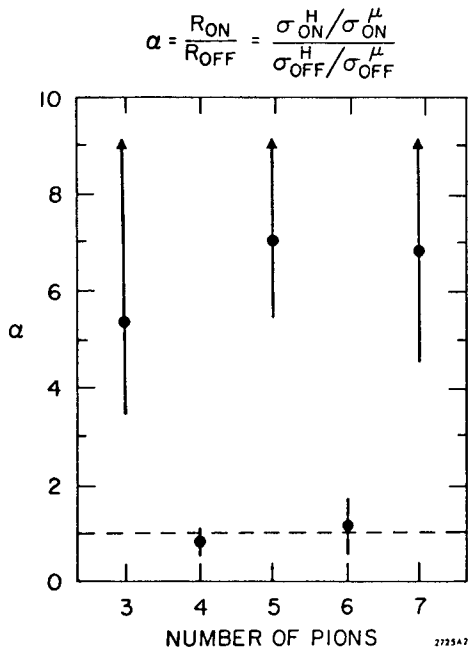
Fig. 10 Comparison of the ratio of multipion to $\mu^{+}\mu^{-}$-pair production at the $\psi(3095)$ (ON) and at 3.0 GeV (OFF).

Fig. 11 Dalitz plot for the $\pi^{+}\pi^{-}\pi^{0}$ decay of the $\psi(3095)$.

$\psi(3095) \rightarrow \pi^{+}\pi^{-}\pi^{0}$
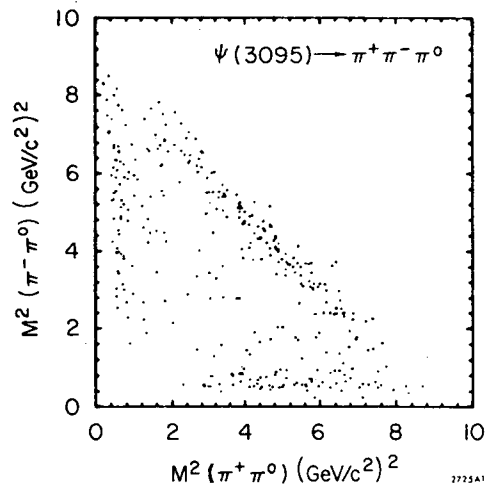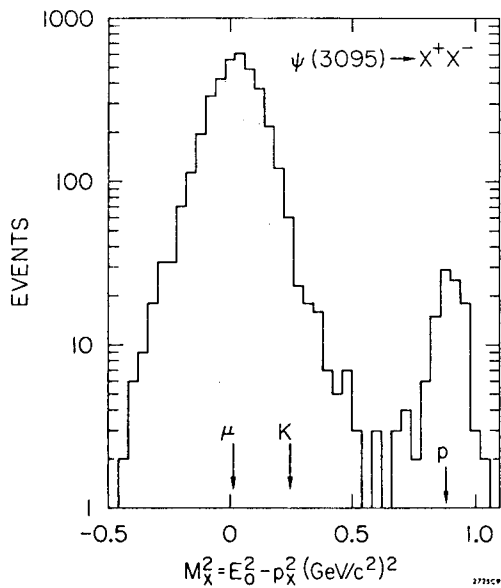
Fig. 12 Mass squared measured as $M_x^2 = E_{beam}^2 - p_x^2$ for collinear 2-prong events at the $\psi(3095)$. e^+e^- pairs have been eliminated by a cut on the shower counter pulse height.

Fig. 13 Momentum of the Λ versus the momentum of the $\bar{\Lambda}$ for 4-prong events compatible with $\psi \rightarrow \Lambda\bar{\Lambda} + x$.
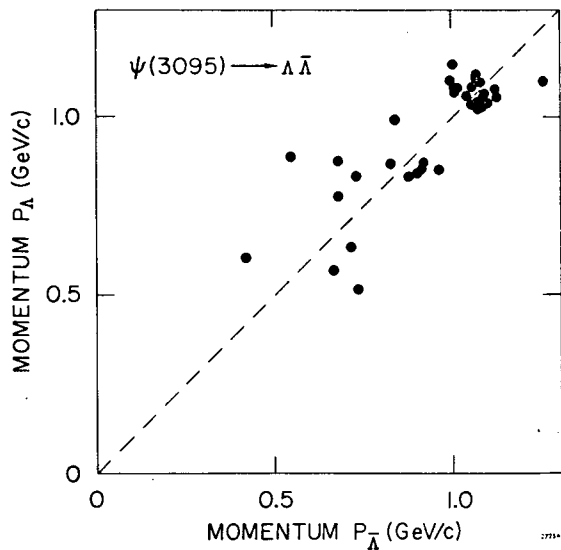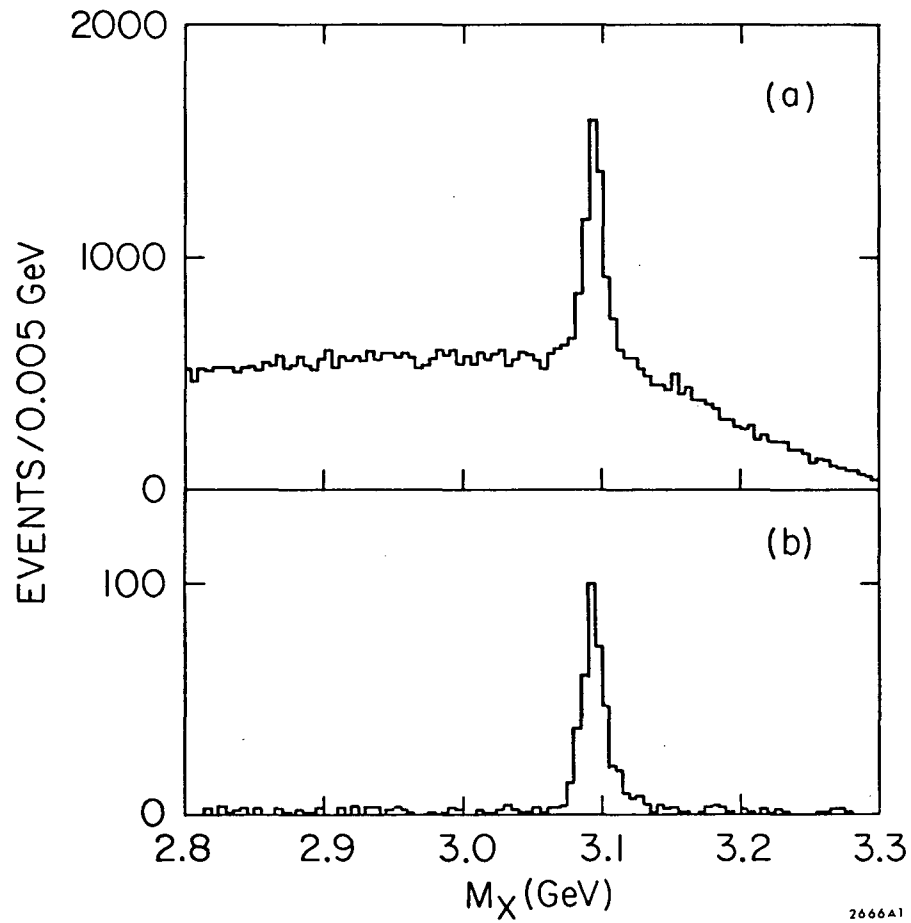
Fig. 14 Invariant mass M_X recoiling against all pairs of oppositely charged particles

a) for all multiprong events.
b) for those events in which the observed charged particles satisfy, within errors, conservation of energy and momentum.
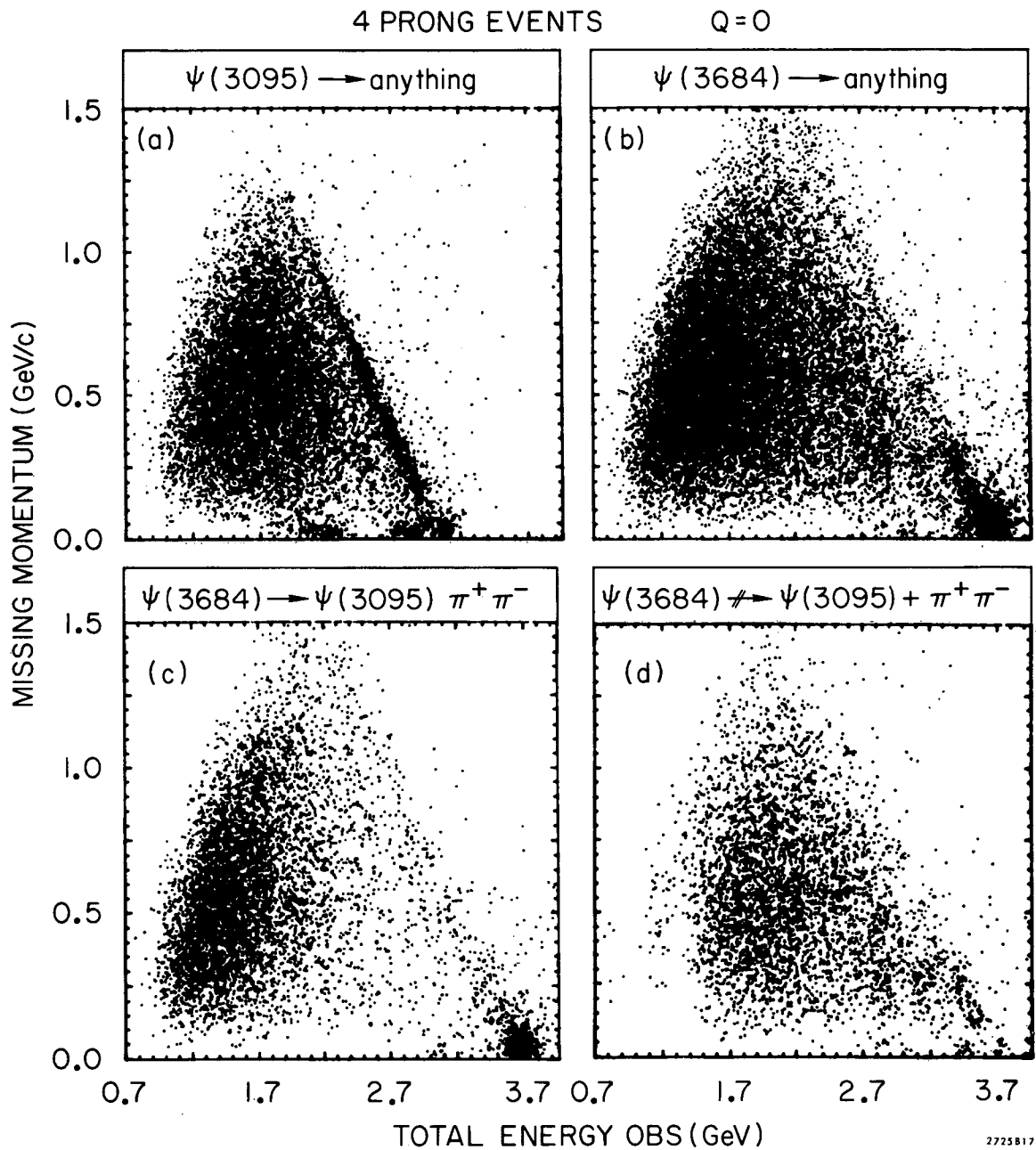
4 PRONG EVENTS   Q = 0

Fig. 15 Comparison of 4-prong events at the $\psi(3095)$ and the $\psi(3684)$. Total momentum versus the sum of the energy of the 4 observed tracks assuming they are all pions.

  a) All 4-prong at $\psi(3095)$.
  b) All 4-prong at $\psi(3684)$.
  c) All 4-prong cascade decays $\psi(3684) \rightarrow \psi(3095) + \pi^+\pi^-$.
  d) All direct decays of the $\psi(3684)$, i.e., cascade decays in (c) removed.